

A Tunable VUV Frequency Comb for ^{229m}Th Nuclear Spectroscopy

CHUANKUN ZHANG^{1,*}, PENG LI², JIE JIANG², LARS VON DER WENSE¹, JOHN F. DOYLE¹, MARTIN E. FERMAN², AND JUN YE¹

¹JILA, National Institute of Standards and Technology and Department of Physics, University of Colorado, Boulder, Colorado, 80309, USA

²IMRA America, Inc., 1044 Woodridge Ave., Ann Arbor, MI 48105, USA

*Corresponding author: chuankun.zhang@colorado.edu

Compiled August 15, 2022

Laser spectroscopy of the ^{229m}Th nuclear clock transition is necessary for the future construction of a nuclear-based optical clock. Precision laser sources with broad spectral coverage in the vacuum ultraviolet are needed for this task. Here, we present a tunable vacuum-ultraviolet frequency comb based on cavity-enhanced 7th-harmonic generation. Its tunable spectrum covers a large fraction of the current uncertainty range of the ^{229m}Th nuclear clock transition. © 2022 Optica Publishing Group

<http://dx.doi.org/10.1364/ao.XX.XXXXXX>

Transitions between metastable nuclear states (isomeric transitions), typically in the X-ray or γ -ray energy range, have been studied extensively with Mössbauer spectroscopy[1]. Recently, quantum control of nuclear excitation[2, 3] has been demonstrated using suitably shaped X-ray pulses. However, high-resolution spectroscopy, and specifically the construction of a nuclear-based optical clock remains an open challenge, mainly due to the lack of narrow-linewidth laser sources in the X-ray range. Among all known nuclear isomeric transitions, ^{229m}Th has a uniquely low excitation energy, suitable for the future construction of a nuclear clock. Recent reviews on this topic can be found in Ref. [4–6]. The ^{229m}Th transition energy has been recently measured to be 8.28 ± 0.17 eV using electron spectroscopy[7] and 8.10 ± 0.17 eV using γ -ray spectroscopy[8]. The transition energy corresponds to a wavelength of about 150 nm in the vacuum-ultraviolet (VUV) spectral region, where table-top narrow-linewidth laser sources are available[9, 10].

The ^{229m}Th nuclear transition is expected to have a long radiative lifetime on the order of 10^3 to 10^4 seconds[11, 12]. This long lifetime corresponds to potentially a high quality factor $Q \approx 10^{20}$, orders of magnitude higher than that in state-of-the-art atomic clocks[13]. Furthermore, due to the small nuclear electromagnetic moments and shielding effects from the electrons, the ^{229m}Th transition is expected to have a low sensitivity to external perturbations. The high quality factor and high resistance to external perturbation make ^{229m}Th a promising candidate for constructing a nuclear optical clock[14, 15]. By applying precision laser measurement tools and coherent quan-

tum control in nuclear physics, a nuclear clock would provide a wide range of new opportunities, including probing the interaction between the electronic shell and the nucleus (e.g. electron bridge effect)[16–19], precise timekeeping with solid-state optical clocks[20–22], and ultrasensitive tests of fundamental physics[23–25].

To develop such a nuclear clock, high-resolution laser spectroscopy of the ^{229m}Th state has to be performed first. There is currently a worldwide effort toward laser spectroscopy of the ^{229m}Th transition employing different laser systems. Nanosecond VUV laser pulses generated via resonant-enhanced four-wave mixing processes are used in the group of E. Hudson at UCLA[26, 27] and the group of E. Peik at PTB[5]. The pulsed VUV laser systems offer broadband tuning range and are suitable for the initial transition search. Full repetition rate frequency combs in the VUV can be generated using femtosecond enhancement cavities[10, 28, 29]. Such VUV frequency comb systems are used in the group of T. Schumm at TU Wien[5, 30] and our group at JILA[31], and are currently being developed for the group of P. Thirolf at LMU[5]. The equidistant narrow frequency comb lines are used to scan for the ^{229m}Th transition in parallel with high spectral resolution. Once the transition is found, a nuclear clock can be directly constructed by stabilizing the comb to the nuclear transition frequency.

We propose to perform direct VUV frequency comb spectroscopy[32] of the ^{229m}Th state using the 7th harmonic of a Yb fiber frequency comb[22]. A remaining challenge is that the typical bandwidth of a VUV comb is significantly smaller than the current uncertainty range of the ^{229m}Th transition[4, 10]. Here we present a tunable VUV frequency comb based on a tunable Yb-fiber oscillator and amplifier system to mitigate this problem. The tunability of the comb allows us to cover a large fraction of the ^{229m}Th transition uncertainty range in several tuning steps.

The tunable Yb-fiber comb layout is shown in Fig. 1 (a). We implement a low-noise 75 MHz Yb-fiber oscillator[33] and amplify its output in cascaded linear (PM-YSF) and nonlinear (PLMA-YDF-25/250) similariton[34] amplifiers. The output of the nonlinear amplifier gives us a coherent broadband infrared frequency comb for seeding the final-stage high-power fiber amplifier. A fraction (10%) of the nonlinear amplifier output is sent to a highly nonlinear photonic crystal fiber (HNLF PCF) for su-

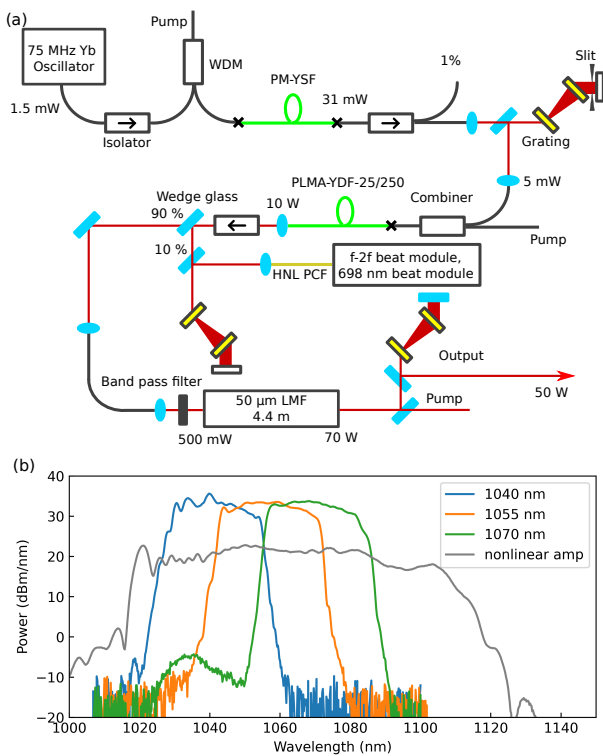


Fig. 1. (a) Tunable Yb-fiber frequency comb. Black lines represent passive fibers. Green lines represent active fiber amplifiers. Red lines are free-space laser paths. Grating pairs (yellow) are used for temporal compression of the laser pulses. A slit is used in combination with the first grating pair to clean up the spectral output from the oscillator. WDM, wavelength-division multiplexer; PM-YSF, polarization-maintaining Yb-doped single-clad fiber; PLMA-YDF-25/250, polarization-maintaining large-mode-area Yb-doped double-clad fiber with 25/250 μm core/cladding diameter; HNL PCF, highly nonlinear photonic-crystal fiber; and LMF, large-mode-area fiber module with 50 μm core diameter. (b) Spectra of the nonlinear similariton amplifier and LMF amplifier output at different wavelength settings.

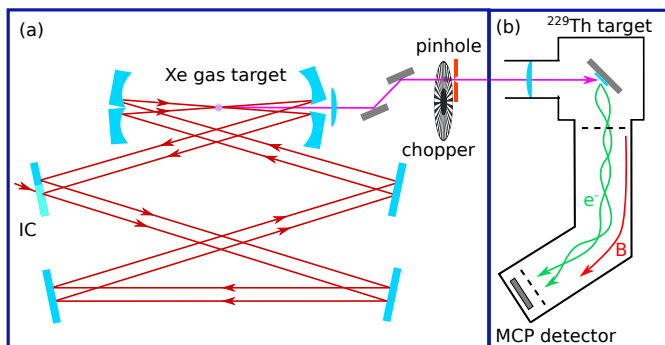


Fig. 2. VUV generation and spectroscopy setup. (a) VUV generation chamber. Detailed description of the noncollinear cavity is presented in Ref. [31]. IC: input coupler. (b) Illustration of spectroscopy setup using a solid-state ^{229}Th target. The green traces (e^-) illustrate the electron trajectory guided by a curved magnetic field (B, red trace). MCP: microchannel plate.

percontinuum generation. We stabilize the comb carrier-envelope offset frequency f_{ceo} by the f-2f self-referencing scheme. To fully stabilize the frequency comb structure, we also phase lock one of the comb lines in the supercontinuum to the Sr clock laser at 698 nm[35]. To achieve the desired spectral tunability of the comb, we select a part of the spectrum from the nonlinear amplifier output using an interference bandpass filter. We can tune the central wavelength continuously from 1040 nm to 1070 nm by changing the angle of the bandpass filter. The filtered light is amplified further in a large-mode-area fiber (LMF) power amplifier. The optical spectra of the nonlinear amplifier and the power amplifier at several different wavelength settings are shown in Fig. 1 (b). The spectral filtering and subsequent amplification allow us to mitigate nonlinear self phase modulation in the LMF fiber and obtain high output spectral power. After the final grating compressor, we produce an infrared frequency comb with $>50\text{W}$ average power and $<150\text{ fs}$ pulse duration.

The output of this high-power infrared frequency comb is then coherently coupled into a femtosecond enhancement cavity for 7th harmonic generation[10], see Fig. 2(a). This cavity provides an enhancement factor of about 100 for the comb peak and average power, which is necessary for driving the 7th harmonic generation efficiently at the original comb repetition rate. We use a crossed-beam geometry[31] to extract the generated harmonics efficiently.

While the noncollinear geometry offers high outcoupling efficiency for high-order harmonics, we estimate the extraction efficiency of the 7th harmonic to be only about 30% based on numerical simulations[31]. As we only need the 7th harmonic for the nuclear spectroscopy experiment, alternative outcoupling methods[10] should be considered. A standard method for cavity-enhanced high harmonic outcoupling is using an intracavity plate at the Brewster angle (Brewster plate) for the fundamental light. Conventional Brewster plate materials like MgO offer up to 2% coupling efficiency for the 7th harmonic, which is rather low[10, 36]. Using nanogratings etched on top of a high reflector, 3% of the 7th harmonic can get diffracted out[37]. Thin plates with high-reflection coatings for the VUV light have been demonstrated before, offering up to 75% reflectivity[38]. However, in long-term operation, they suffer from degradation caused by UV irradiation. A thin plate with antireflection coatings for s-polarized fundamental light at a grazing incidence angle (Grazing Incidence Plate, GIP) was also proposed for XUV-outcoupling[39]. Using 70 degrees incidence angle, a coupling efficiency of 40% is feasible. However, this technique has not yet been tested in an intra-cavity setup.

Table 1 summarizes different outcoupling methods discussed above for the intra-cavity generated 7th harmonic.

Table 1. Outcoupling methods for 7th harmonic

Methods	Efficiency	Challenge
Noncollinear	30%	Alignment complexity
Brewster plate	2%	Low efficiency
XUV grating	3%	Low efficiency
XUV HR plate	75%	Degradation
GIP	40%	No intracavity test

In the detection system, shown in Fig. 2 (b), a thin 10 nm film of thorium oxide coating on a platinum-coated Si wafer will be

used as the target for the spectroscopy. In the internal-conversion decay process, the excited nuclear state decays dominantly by transferring its energy to an electron instead of emitting a photon. The nuclear transition linewidth is thus broadened by this additional decay channel to about 16 kHz [40]. Using the solid-state target allows us to irradiate 10^{13} nuclei in parallel. We plan to perform fast and low-noise detection of the nuclear isomeric decay events by observing the internal-conversion electrons emitted from the surface using a microchannel plate detector.

As described in Ref. [22], we plan to use gated pulses to excite the nuclear transition and synchronously detect the isomeric decay events after the laser is turned off. This detection scheme requires a short laser turnoff time compared to the isomeric lifetime of 10 μ s. Furthermore, the intracavity Xe plasma generated by the laser causes a VUV fluorescent afterglow lasting on the order of tens of μ s [41], which would potentially lead to an increased background for the spectroscopy measurement. We focus the VUV laser through a 100 μ m diameter copper pin-hole and implement an in-vacuum chopper wheel running at 30,000 revolutions per minute to gate the laser. The chopper wheel system allows us to achieve clean laser gating with sub-microsecond on-off times. Furthermore, we use a magnetic field to guide the electrons to avoid a direct line-of-sight between the target and the microchannel plate detector, see Fig. 2 (b). Using this detection system, we reduce the laser-induced background in the nuclear spectroscopy to a negligible amount compared to the background from intrinsic target radioactivity, which is the main source of background.

To drive the $^{229\text{m}}\text{Th}$ nuclear transition efficiently, the VUV frequency comb linewidth should be comparable to or narrower than the transition linewidth. We quantify the laser linewidth by integrating the phase noise starting from a 1 MHz Fourier frequency [42]. It has been experimentally verified that in the cavity-enhanced harmonic generation processes, just like in other noise-free harmonic generation processes, the phase noise power spectral density (PSD) scales as $S_{\phi}(f) \propto q^2$, where q is the harmonic order [43]. In our case for the 7th harmonic generation, this scaling poses a 49 times more stringent requirement of the phase noise PSD on the fundamental comb.

To characterize the comb linewidth, we measure the phase noise of the Yb-fiber comb by stabilizing it to a 1064 nm low-noise reference laser and measuring its in-loop phase noise PSD. The comb f_{ceo} is simultaneously stabilized to a radio-frequency reference. In addition to the power enhancement, the optical cavity also filters the high-frequency optical phase noise due to its narrow resonance linewidth. Using the phase noise scaling relation and a cavity finesse of 400, we can scale the optical phase noise of the fundamental comb to the phase noise of the 7th harmonic comb, shown in Fig. 3. The root-mean-squared integrated phase noise of the beat note remains only 0.022 rad down to 10 Hz. This corresponds to an integrated phase noise of only 0.15 rad in its 7th harmonic, and thus $> 97\%$ optical power remaining in the coherent VUV frequency comb teeth of 10 Hz linewidth. Additional phase noise on the 7th harmonic from intensity noise via the intensity-dependent dipole phase is negligible [43]. We estimate that the linewidth of our 7th harmonic would be limited to kHz level due to optical path length fluctuations in our experiment setup, which is still narrow compared to the internal-conversion broadened nuclear transition linewidth of 16 kHz.

We show several measured fundamental Yb-fiber comb spectra in Fig. 4 (a) under different wavelength settings. The corresponding VUV frequency comb spectra, measured using a

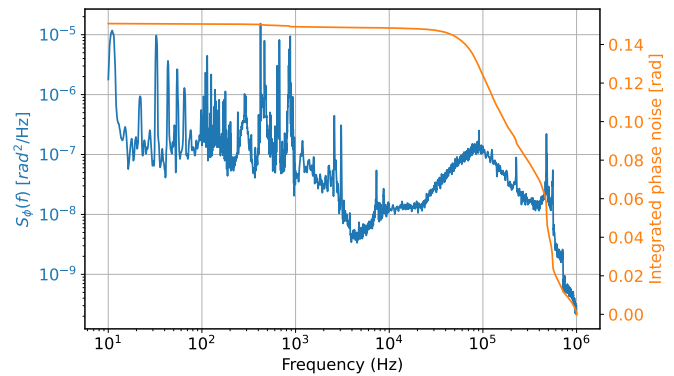


Fig. 3. Phase noise performance of the VUV comb. A low-pass filtering function (corner frequency: 93.75 kHz) corresponding to the transfer function of our enhancement cavity has been applied, which reduces the high-frequency phase noise. The left axis is for phase noise power spectral density (blue curve), and the right axis for the integrated phase noise (orange curve) integrated from 1 MHz down to the corresponding value of the x-axis.

grating-based spectrometer (HP Spectroscopy, easyLIGHT) with < 0.1 nm resolution, are shown in Fig. 4(b). We estimate the VUV power per comb line to be about 1 nW delivered onto the target, sufficient for the nuclear transition search [22]. Given the limited spectral coverage of the VUV frequency comb at each setting, we need to tune the central comb wavelength in fine steps to cover a large fraction of the uncertainty range of the $^{229\text{m}}\text{Th}$ nuclear transition. The tunable comb was initially designed to cover the energy range given in Ref. [7] before the publication of Ref. [8]. Using a longer fiber in the final stage amplifier can potentially shift the spectral coverage to longer wavelengths given in Ref. [8].

In conclusion, we have constructed a tunable VUV frequency comb dedicated to our $^{229\text{m}}\text{Th}$ nuclear spectroscopy. The tuning implemented in the Yb-fiber comb amplifier system allows us to easily tune the VUV spectrum over a large fraction of the $^{229\text{m}}\text{Th}$ nuclear transition uncertainty range, significantly improving our chance of finding the nuclear clock transition. Furthermore, once the clock transition is found, the VUV comb structure can serve directly as the clockwork for reading out the transition frequency and constructing a solid-state nuclear clock referenced to our existing Sr optical atomic clock.

Funding. This work is supported by ARO Grant No. W911NF2010182, AFOSR Grant No. FA9550-19-1-0148, NSF Grant No. PHY-1734006 and National Institute of Standards and Technology

Acknowledgments. We thank J. Weitenberg, A. Ozawa, O. Pronin, A. L. Gaeta, Y. Okawachi, P. St.J. Russell, F. Tani, J. Lampen, J. S. Higgins and L. R. Liu for helpful discussions. Lars v.d.Wense acknowledges support from the Alexander von Humboldt Foundation.

Data availability. Data underlying the results presented in this paper are not publicly available at this time but may be obtained from the authors upon reasonable request.

REFERENCES

1. N. N. Greenwood, *Mössbauer spectroscopy* (Springer Science & Business Media, 2012).

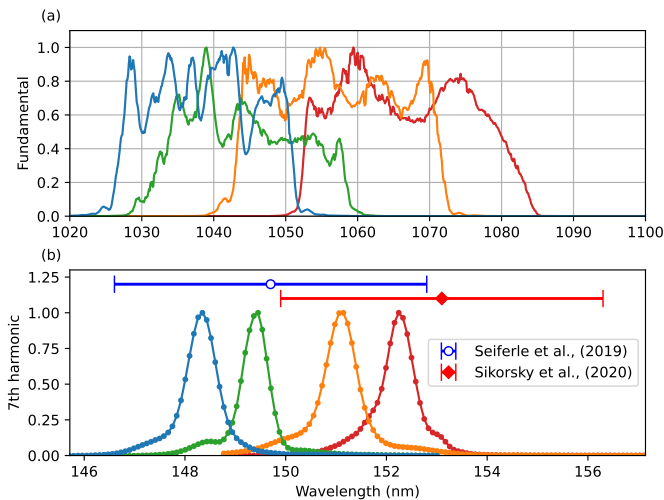


Fig. 4. Comb tunability. (a) Fundamental comb spectrum, measured as the leakage transmission from one of the enhancement cavity mirrors. (b) VUV spectrum of the outcoupled harmonics, measured with a grating-based VUV spectrometer. Horizontal error bars indicate the $^{229\text{m}}\text{Th}$ transition uncertainty ($1\text{-}\sigma$) ranges given in Seiferle et al.[7] and Sikorsky et al.[8]. We obtain similar overall VUV powers at each wavelength setting. Vertical scales in the plots are normalized to unity.

2. T. J. Bürvenich, J. Evers, and C. H. Keitel, *Phys. Rev. Lett.* **96**, 142501 (2006).
3. K. P. Heeg, A. Kaldun, C. Strohm, C. Ott, R. Subramanian, D. Lentrodt, J. Haber, H.-C. Wille, S. Goerttler, R. Ruffer *et al.*, *Nature* **590**, 401 (2021).
4. L. von der Wense and B. Seiferle, *The Eur. Phys. J. A* **56**, 1 (2020).
5. E. Peik, T. Schumm, M. Safronova, A. Pálffy, J. Weitenberg, and P. G. Thirolf, *Quantum Sci. Technol.* **6**, 034002 (2021).
6. K. Beeks, T. Sikorsky, T. Schumm, J. Thielking, M. V. Okhapkin, and E. Peik, *Nat. Rev. Phys.* **3**, 238 (2021).
7. B. Seiferle, L. von der Wense, P. V. Bilous, I. Amersdorffer, C. Lemell, F. Libisch, S. Stellmer, T. Schumm, C. E. Düllmann, A. Pálffy *et al.*, *Nature* **573**, 243 (2019).
8. T. Sikorsky, J. Geist, D. Hengstler, S. Kempf, L. Gastaldo, C. Enss, C. Mokry, J. Runke, C. E. Düllmann, P. Wobrauschek *et al.*, *Phys. Rev. Lett.* **125**, 142503 (2020).
9. W. Ubachs, K. Eikema, W. Hogervorst, and P. Cacciani, *JOSA B* **14**, 2469 (1997).
10. I. Pupeza, C. Zhang, M. Högner, and J. Ye, *Nat. Photonics* **15**, 175 (2021).
11. E. Tkalya, C. Schneider, J. Jeet, and E. R. Hudson, *Phys. Rev. C* **92**, 054324 (2015).
12. N. Minkov and A. Pálffy, *Phys. Rev. Lett.* **122**, 162502 (2019).
13. T. Bothwell, C. J. Kennedy, A. Aeppli, D. Kedar, J. M. Robinson, E. Oelker, A. Staron, and J. Ye, *Nature* **602**, 420 (2022).
14. E. Peik and C. Tamm, *Europhys. Lett.* **61**, 181 (2003).
15. C. J. Campbell, A. G. Radnaev, A. Kuzmich, V. A. Dzuba, V. V. Flambaum, and A. Derevianko, *Phys. Rev. Lett.* **108**, 120802 (2012).
16. E. Tkalya, *Sov. J. Nucl. Phys.* **55**, 1611 (1992).
17. S. Porsev, V. Flambaum, E. Peik, and C. Tamm, *Phys. Rev. Lett.* **105**, 182501 (2010).
18. F. Karpeshin and M. Trzhaskovskaya, *Phys. Rev. C* **95**, 034310 (2017).
19. P. V. Bilous, H. Bekker, J. C. Berengut, B. Seiferle, L. von der Wense, P. G. Thirolf, T. Pfeifer, J. R. C. López-Urrutia, and A. Pálffy, *Phys. Rev. Lett.* **124**, 192502 (2020).
20. W. G. Rellergert, D. DeMille, R. Greco, M. Hehlen, J. Torgerson, and E. R. Hudson, *Phys. Rev. Lett.* **104**, 200802 (2010).
21. G. Kazakov, A. Litvinov, V. Romanenko, L. Yatsenko, A. Romanenko, M. Schreitl, G. Winkler, and T. Schumm, *New J. Phys.* **14**, 083019 (2012).
22. L. von der Wense and C. Zhang, *The Eur. Phys. J. D* **74**, 1 (2020).
23. P. G. Thirolf, B. Seiferle, and L. von der Wense, *Annalen der Physik* **531**, 1800381 (2019).
24. A. Banerjee, H. Kim, O. Matsedonskyi, G. Perez, and M. S. Safronova, *J. High Energy Phys.* **2020**, 1 (2020).
25. P. Fadeev, J. C. Berengut, and V. V. Flambaum, *Phys. Rev. A* **102**, 052833 (2020).
26. J. Jeet, "Search for the low lying transition in the ^{229}Th nucleus," Ph.D. thesis, University of California, Los Angeles (2018).
27. L. C. von der Wense, B. Seiferle, C. Schneider, J. Jeet, I. Amersdorffer, N. Arlt, F. Zacherl, R. Haas, D. Renisch, P. Mosel *et al.*, *Hyperfine Interactions* **240**, 1 (2019).
28. R. J. Jones, K. D. Moll, M. J. Thorpe, and J. Ye, *Phys. Rev. Lett.* **94**, 193201 (2005).
29. C. Gohle, T. Udem, M. Herrmann, J. Rauschenberger, R. Holzwarth, H. A. Schuessler, F. Krausz, and T. W. Hänsch, *Nature* **436**, 234 (2005).
30. J. Seres, E. Seres, C. Serrat, E. Young, J. Speck, and T. Schumm, *Opt. Express* **27**, 6618 (2019).
31. C. Zhang, S. B. Schoun, C. M. Heyl, G. Porat, M. B. Gaarde, and J. Ye, *Phys. Rev. Lett.* **125**, 093902 (2020).
32. A. Cingöz, D. C. Yost, T. K. Allison, A. Ruehl, M. E. Fermann, I. Hartl, and J. Ye, *Nature* **482**, 68 (2012).
33. Y. Li, N. Kuse, A. Rolland, Y. Stepanenko, C. Radzewicz, and M. E. Fermann, *Opt. Express* **25**, 18017 (2017).
34. M. E. Fermann, V. Thomsen, J. M. Dudley, and J. D. Harvey, *Phys. Rev. Lett.* **84**, 6010 (2000).
35. E. Oelker, R. Hutson, C. Kennedy, L. Sonderhouse, T. Bothwell, A. Goban, D. Kedar, C. Sanner, J. Robinson, G. Marti *et al.*, *Nat. Photonics* **13**, 714 (2019).
36. E. D. Palik, *Handbook of optical constants of solids*, vol. 3 (Academic press, 1998).
37. D. Yost, T. Schibli, and J. Ye, *Opt. Lett.* **33**, 1099 (2008).
38. A. Ozawa, Z. Zhao, M. Kuwata-Gonokami, and Y. Kobayashi, *Opt. Express* **23**, 15107 (2015).
39. O. Pronin, V. Pervak, E. Fill, J. Rauschenberger, F. Krausz, and A. Apolonski, *Opt. Express* **19**, 10232 (2011).
40. B. Seiferle, L. Von Der Wense, and P. G. Thirolf, *Phys. Rev. Lett.* **118**, 042501 (2017).
41. M. Jinno, H. Kurokawa, M. Aono, and H. Ninomiya, *Czechoslov. J. Phys.* **50**, 433 (2000).
42. J. Hall and M. Zhu, "An introduction to phase-stable optical sources," in *International School of Physics Enrico Fermi Course CXVII, Laser Manipulation of Atoms and Ions*, E. Arimondo, W. Phillips, and F. Strumia, eds. (North Holland, CH, 1992), pp. 671–701.
43. C. Benko, T. K. Allison, A. Cingöz, L. Hua, F. Labaye, D. C. Yost, and J. Ye, *Nat. Photonics* **8**, 530 (2014).